

Impact of pointing performance on the optical downlink for the Optical Payload for Lasercomm Science (OPALS) system

Results from pre-flight laboratory testing

Bogdan V. Oaida, Michael Kokorowski, Kenneth S. Andrews, Marcus Wilkerson
Jet Propulsion Laboratory
California Institute of Technology
Pasadena, California, United States of America
bogdan@jpl.nasa.gov

Baris I. Erkmen
Google Inc.,
Mountain View, California, United States of America.
erkmen@google.com

William Wu
Quantitative Engineering Design, Inc.
Berkeley, California, United States of America
w@qe-design.com

Abstract—The Optical Payload for Lasercomm Science (OPALS), developed at JPL, is a technology demonstration project which is set to begin operations from the International Space Station in early 2014. Its goal is to demonstrate the feasibility of an optical communication link from low-Earth orbit (LEO), i.e. the ISS, to a ground terminal located at JPL's Optical Communications Telescope Laboratory (OCTL). Pointing performance is a key consideration, and often a driver, in the design of space-to-ground optical communications links, as was the case for our project. In this paper we discuss how the allocations for the pointing system were derived and the impact of the pointing performance on the optical downlink. We address the contributions from static and quasi-static pointing offsets (bias) as well as those from the fast-dynamic disturbances produced by the two-axis gimbal and control loop (jitter). Results from laboratory testing are presented and compared to the requirements.

Keywords—OPALS; optical communications; lasercomm; pointing jitter; pointing bias; ISS disturbance

I. INTRODUCTION

The Optical Payload for Lasercomm Science (OPALS) developed at JPL is a technology demonstration project which is set to begin operations from the International Space Station in the spring of 2014 [1]. Its goal is to demonstrate the feasibility of an optical communication link from low-Earth orbit (LEO), i.e. the ISS, to a ground terminal located at JPL's Optical Communications Telescope Laboratory (OCTL).

OPALS has been under development at JPL since 2009. As an ultra-low cost project, it made extensive use of COTS and lab-grade components. This approach resulted in an unconventional, yet innovative, design which took advantage of the generous mass and power capabilities of the

International Space Station (ISS) [2]. OPALS completed the end-to-end ground testing of its optical link at JPL in June 2013.

OPALS will be JPL's first space-borne lasercomm terminal and NASA's first on the ISS. The payload is launched aboard a SpaceX Falcon9 Dragon vehicle from Cape Canaveral Air Force Station. After being installed externally on the ISS, OPALS plans to operate for a minimum of 90 days, during which it aims to perform dozens of downlinks at a nominal rate of 50 Mbps. These downlinks will provide valuable information about the effects of atmospheric- and pointing-induced fades on link quality, as well as test various pointing strategies for acquiring and tracking the ground station using a ground-generated beacon.

The space-borne element of OPALS, referred to as the Flight System or Payload, is shown in Fig. 1. The design of the Flight System, its components, along with the larger OPALS architecture and the concept of operations have been described elsewhere [2]. Reference [3] provides additional information on the design of the optical links and the motivation behind the chosen architecture.

This paper further elaborates on the aspects of the pointing design and its impact on the optical downlink performance, which previously have only been touched on briefly [2, 3]. The remainder of the paper is organized as follows. Section II provides a description of how pointing losses are bookkept in the downlink budget and a key trade performed to identify the appropriate allocation. In section III we describe results from laboratory testing of the pointing performance. In particular, we will discuss the pointing-induced power fluctuations at the receiver, and the calibration algorithms between flight and

All work described in this paper was carried out at the Jet Propulsion Laboratory, California Institute of Technology, under a contract with the National Aeronautics and Space Administration. Baris I. Erkmen's contributions to the writing of this paper was done at Google Inc. William Wu's contributions to the writing of this paper was done at Quantitative Engineering Design™, Inc.



Fig. 1. OPALS payload in flight configuration during integration with the launch vehicle. The two-axis gimbal-mounted optical transceiver (shown here with a protective cover on) and the barrel-shaped seal container give OPALS its distinctive look.

ground terminals. Lastly, in section IV we summarize our conclusions.

II. DESIGN CONSIDERATIONS FOR POINTING PERFORMANCE

As with any free-space optical communications link, accurate and precise pointing of the laser beam is a leading consideration in the design of the system. The beam must not only be pointed sufficiently close to the targeted receiver, i.e. minimize the offset, to ensure good power margin, but must also exhibit good stability for the duration of the link so as to minimize pointing-induced fades and prevent loss-of-lock. It therefore follows that one way to specify the total allowable pointing loss is in terms of the contribution from the quasi-static offset and the dynamic disturbances to which the transmitter is subjected to. In this paper, we refer to these two sources of pointing losses as bias and jitter, respectively.

Since known offsets between the transmit and receive paths can often be calibrated out, the bias in this case is the offset knowledge residual. For OPALS this term is driven by the accuracy with which the alignment of the two optical axes can be measured in the lab, and by shifts that may occur due to launch vibrations and thermal cycling-induced stresses.

The beam jitter occurs about the bias and is primarily a function of the inherent performance of the pointing system (i.e. the OPALS gimbal) and the disturbance environment of the platform on which the pointing system is mounted (i.e. the ISS). The former can be minimized by careful design of the gimbal and selection of the actuators with good jitter performance such as stepper motors. Minimizing the platform contribution requires knowledge of the disturbance power spectral density so that the control loop can reject the disturbance over a wide spectrum [4].

The pointing performance required to establish connectivity in free-space optical communication downlinks from low-Earth

orbit prohibit open-loop pointing strategies. Therefore, OPALS employs a receiver-sourced beacon as an acquisition and tracking reference. A camera co-aligned to the downlink beam images the beacon and a control system closes the loop around it.

One key design consideration is the balancing act between having a downlink beam that is wide enough to accommodate acceptable mispoint losses but not so wide that it cannot deliver sufficient power to the ground detector to maintain lock. This balancing act can be achieved by optimizing the effective isotropic radiated power (EIRP)—in this case defined as the product of the transmitted power, the transmitter efficiency and the optical aperture gain—for a given combination of beam divergence and mispoint angle allocation. Since the OPALS Flight System uses a coarse pointing gimbal, (i.e. no fast steering mirror) it requires a wider beam and sufficient optical power to satisfy the photon budget. Fig. 2 shows the beam divergence that would maximize the EIRP for a set of mispoint angles given an optical power output of 0.83 W—the minimum the design was required to achieve. It can be seen that as the system is allowed to incur larger mispoint-induced losses, the maximum achievable EIRP is reduced and the minimum divergence required increases. As indicated by the black circle in this figure, OPALS chose a design that ensured the link could be closed given a conservative estimate of the mispoint allocation, primarily based on the anticipated gimbal motor performance. The expected operational performance, denoted by the green diamond, is derived from test data and exceeds the design requirement, largely due to both better-than-expected power output (2.01 W) and pointing stability of the closed loop control system.

For OPALS, the total mispoint allocation was 525 μrad . Given that the beam divergence (measured at the $1/e^2$ level) was just over 1 milliradian, the system could be off-pointed by as much as half the beam width and still have a high

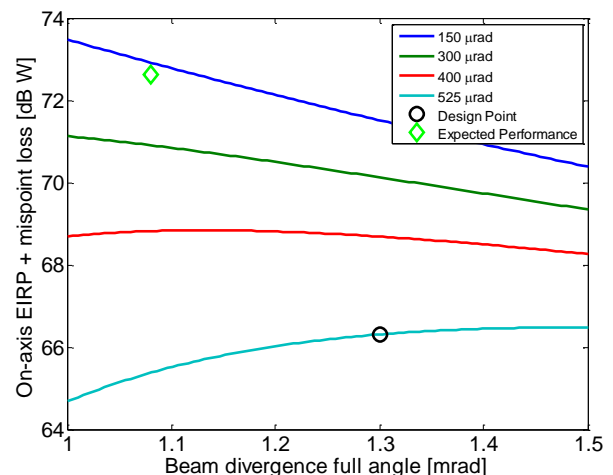


Fig. 2. Performance space of the optical downlink shows the sensitivity to beam divergence for a number of mispoint allocations (lines) as well as the design point (circle) and the expected performance derived from testing (diamond). The transmitted optical power used for this calculation is the requirement-specified 0.833 W, except for the expected performance which uses 2.01 W, per the value measured during testing.

probability of maintain lock with the ground detector. This probability is determined, in part, by how the mispoint angle is sub-allocated between jitter and bias. OPALS aimed to maximize the allocation for jitter due to uncertainty in the performance of the actuators early on in the design process. Higher jitter, however, also means that the downlink beam is more susceptible to pointing-induced fades, and consequently could lead to frequent loss of lock. Fig. 3 shows that, for a mispoint allocation of 525 μrad , the probability of these fades occurring increases dramatically if the jitter fraction makes up more than approximately 0.8 of the total allocation. OPALS required a pointing-induced fading probability no greater than 2.7×10^{-3} which resulted in a jitter contribution allocation of 375 μrad , 3σ , (~ 0.7 of the total mispoint angle allocation), and a bias contribution allocation of 150 μrad . As will be shown in the next section, meeting the bias allocation proved to be more challenging than meeting the jitter allocation.

III. POINTING PERFORMANCE TESTING

The focus of this section is to provide an overview of OPALS testing performed with the goal of verifying the pointing performance at the integrated system level. This testing focused on maintaining the downlink beam on the ground receiver in the presence of external disturbance. The ability of the Flight System to locate and acquire the beacon will not be discussed at length in this paper—beyond establishing the minimum threshold for detection—as it is largely independent of the OPALS link design and more a function of the open-loop pointing strategy employed by the Flight System, a topic that is left for discussion in a future publication. Instead, here we will focus on describing how we tested the closed-loop tracking performance of the Flight System, as this had large implications on the downlink losses attributed to pointing induced fades. We will then describe the in-lab testing of a critical method for determining pointing bias between the Flight System transmit and receive apertures with a Ground System emulator. This test verified that a quasi-static misalignment that may arise due to post-launch drifts in the transmit-receive boresight can be measured from the ground and can be largely compensated for in the downlink pointing control.

These tests were conducted under the most-flight like conditions that could be simulated in the laboratory setting given cost and time constraints. The most significant of these conditions was the presence of the external disturbance in the azimuth axis. The most significant environmental condition absent from the test was the anticipated non-uniform background at 976nm. However, because OPALS has designed the uplink beacon with significant power margin, it is anticipated that identifying and isolating the beacon will not be limited by background radiation incident on the photodetector [3]. A backup plan in the event of unexpected sensitivity to background radiation is to pursue night-time operations, which constitute approximately 50% of predicted downlink opportunities.

Prior to presenting the results, a discussion of the test is required. At one end of the setup, the Ground System receiver was emulated with bench-mounted optics to focus the 1550nm laser beam delivered by the Flight System on to the

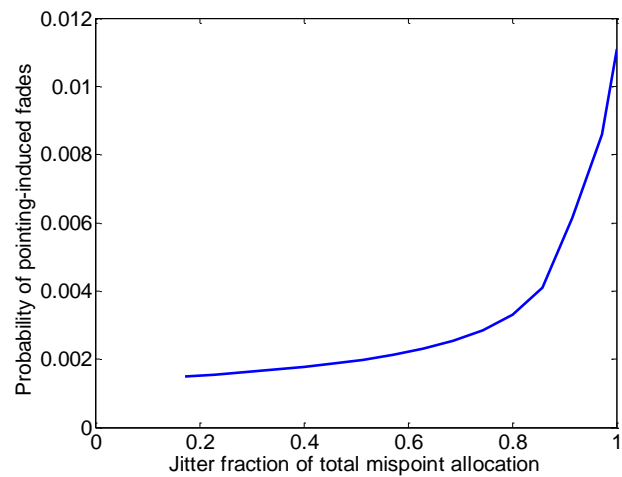


Fig. 3. Probability of pointing-induced fade increases as jitter increases relative to bias for the same pointing loss allocation (in this case 525 μrad). The OPALS design aimed for a jitter fraction of ~ 0.7 or lower, and achieved as good as 0.13 during testing.

detector/receiver assembly that would later be integrated to the OCTL telescope. The emulator also produced a collimated 976nm beacon that overfilled the Flight System camera aperture for the flight terminal to track.

The Ground System emulator was about 20 feet away from a second optics bench which accommodated the two main Flight System assemblies: the sealed container housing the laser and avionics and the optical head integrated to gimbal assembly. The gimbal was mounted on top of a single-axis rotary stage (Fig. 4) which was used to impart velocity profiles typical of the ones the gimbal will have to track against when installed on the ISS in order to remain pointed at the Ground System. Thus by commanding the gimbal to track the beacon while the rotary stage moved, we were able to create the same relative geometry which will be seen during operations by the

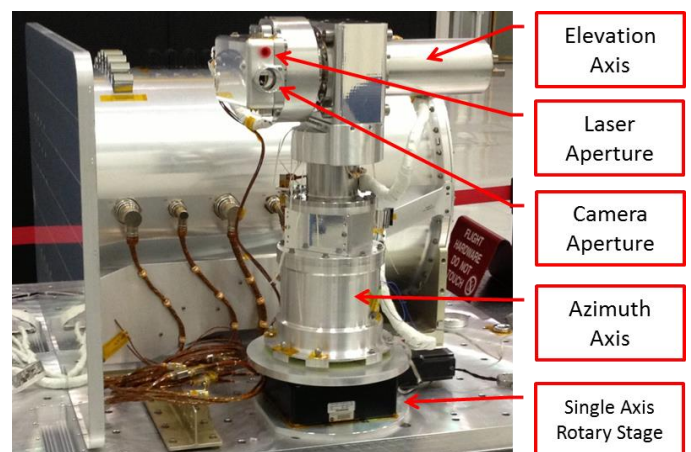


Fig. 4. Optical gimbal assembly mounted on the single axis rotary stage to enable closed-loop testing of the azimuth axis using flight-like ISS angular velocity profiles.

azimuth axis. Given the limitations of the setup, the elevation axis of the gimbal could not be externally stimulated. While this is less than ideal, it is not completely unlike some flight geometries, many of which provide high-elevation passes (from the ground receiver perspective) that require minimal actuation of the elevation axis of the gimbal. It is therefore expected that the total disturbance, calculated as the RSS of the contributions from each axis, is dominated by the slewing of the azimuth axis.

Losses associated with pointing-induced fades are one of the dominant terms in the downlink budget. Furthermore, as illustrated in Fig. 2, the link shows great sensitivity to the relationship between the mispoint allocation and the beam divergence. With the divergence set by the optics, the performance of the link becomes largely dependent on how well pointing losses can be minimized. The total mispoint is defined as the sum of the bias and the 3σ jitter. For OPALS, the jitter was expected to be about twice as large as the bias. Testing of the former is discussed in Section III.A, with the latter being addressed in Section III.B.

A direct measurement of the downlink beam jitter at the receiver was not feasible due to test setup limitations. However, an accurate proxy measurement was achieved by obtaining the residual error of the beacon centroid from camera frames recorded at 100Hz. For a perfectly Gaussian distribution of the error residuals, the 3σ point corresponds to the 99.73% confidence interval, i.e., to having a probability of outage equal to 2.7×10^{-3} . As will be shown, however, the distribution often deviated from Gaussian. Thus, the jitter metric was eventually calculated as the deviation from the center of the beam that yielded the same outage probability, namely 2.7×10^{-3} .

It must be noted at this time that all the results presented here were acquired in the absence of jitter contributions from the ISS platform. To the extent that disturbance was known at the time, its contribution was accounted for analytically via modeling during post-processing of test data. It is predicted that the contribution from the ISS that could not be suppressed

by the OPALS control loop is a few microradians, or a very small fraction of the beam-width. Thus it is anticipated that disturbances introduced by the ISS will not adversely impact the pointing stability of the OPALS optical head.

A. Measured Jitter Performance

One of the first tests performed was to confirm the minimum power required for detection of the beacon by the Flight System, which would enable transition from open-loop searching of the beacon to closed-loop tracking. The irradiance at (or near) the Flight System camera aperture needed by the Flight System algorithm to identify the beacon with sufficient confidence to command transition into closed loop pointing is 120 nW/m^2 . As was shown by others [3], however, the expected minimum irradiance delivered to the Flight System by the ground beacon is $\sim 300 \text{ nW/m}^2$, and thus that was the level used during testing (henceforth referred to as the threshold level). The results obtained indicate that the pointing stability performance at this level is rather poor, particularly for the azimuth axis, as indicated in the left panel of Fig. 5. The histogram shows a bimodal distribution of the centroid error residuals, along with the computed jitter value from both the raw data (i.e. the histogram) and from a Gaussian fit to the data. Although the bimodal behavior is not prominent, it is sufficient to induce unwanted power fluctuations and even temporary fades. It is believed that this behavior is due to a beacon spot size that is smaller than a pixel and thus causing discrete jumps in the centroiding from one pixel to another, i.e. preventing sub-pixel centroiding.

Given the large performance range of the beacon power, it was hypothesized that an increase in brightness could lead to increased tracking performance and thus reduce jitter. More power translates to a larger beacon spot on the CCD which enables smoother tracking and fewer discrete jumps between adjacent pixels. This was indeed the case as is shown in the right panel of Fig. 5. The bimodal behavior exhibited by the azimuth axis is much less pronounced and is all but removed from the elevation axis. By increasing the beacon irradiance

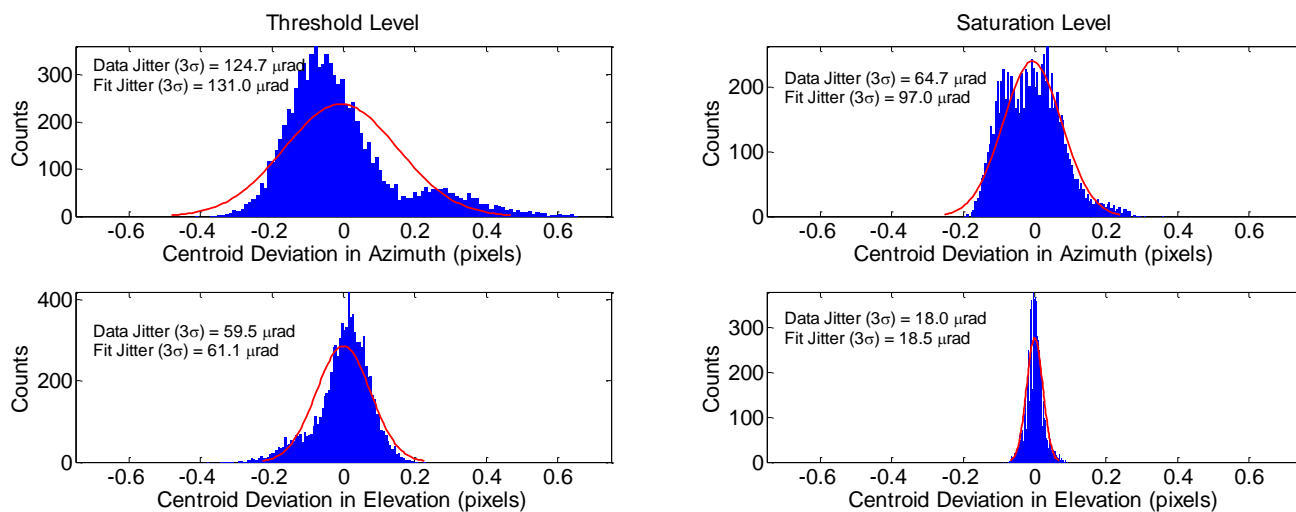


Fig. 5. While the beacon irradiance needed for acquisition threshold [left] is sufficient to meet the jitter requirement, by increasing it up to the point of pixel saturation [right] the requirement can be exceeded by as much as a factor of 4.5. Under the latter, the fit to a Gaussian distribution also improves substantially.

delivered to the flight camera by a factor of four, and reducing the camera gain by a factor of three, the jitter performance improved by a factor of 2.2. These results along with relevant camera settings are shown in TABLE I.

Note that all tests were performed with constant beacon intensity for the duration of each ~110 second simulated pass. During operations the beacon intensity will increase as the distance between the ISS and the OCTL is reduced by almost a factor of two at closest approach before decreasing again as it moves past the ground station. The beacon power will be tuned for each pass to ensure that it stays between the two values listed in TABLE I., thereby ensuring it can always be acquired but will not over-saturate the pixel at any point in a pass.

From Fig. 5 we also see that the distribution of centroid errors have a poor fit to a Gaussian distribution, particularly for the azimuth data. This finding suggests that computing the 3σ value from the fit or the histogram may not give a good indication of the outage performance. Fig. 6 illustrates this with another example obtained from a free-space, closed loop test performed with the beacon irradiance set just above the acquisition threshold. The jitter computed from the histogram yields a value of 130.4 μrad , while computing the jitter from the Gaussian fit yields a value of 148.7 μrad .

A more relevant assessment of the jitter is derived from the deviation that results in an outage probability of 2.7×10^{-3} , which, as discussed at the beginning of Section III, is the outage probability that one would observe with 3σ deviation if the centroid error distribution were truly Gaussian. Thus, the cumulative density function (CDF) of the centroid errors are estimated based on the histograms, and the value (in pixel units) at which this threshold is crossed is identified. Knowing that each pixel is 261.8 μrad , we then calculate the jitter to be 154.9 μrad . These results are displayed in Fig. 7, from which,

TABLE I. BY INCREASING THE BEACON IRRADIANCE FROM THE ACQUISITION THRESHOLD BY A FACTOR OF FOUR, A 2.2X IMPROVEMENT IN POINTING JITTER WAS OBSERVED

Beacon Detection Level	Beacon Irradiance (nW/m^2)	Exposure (msec)	Gain	Flux (DN)	Jitter (μrad)
Acquisition Threshold	~300	10	500	750	138.2
Pixel Saturated	~1200	10	170	760	67.2

in conjunction with Fig. 6, we can determine that the Gaussian fit method underestimates the jitter by approximately 4%, and the jitter computed from the histogram underestimates it by approximately 16%. The requirement of 325 μrad is nevertheless met by more than a factor of two even when the beacon intensity is set at the acquisition threshold.

B. Flight-Ground Calibration

In this section, we discuss the OPALS Flight-Ground Calibration intended to overcome the misalignment between the Flight System tracking camera optical axis and the downlink beam.

For ideal operation, the camera look direction would be exactly co-aligned with the downlink beam. If this ideal case were true, then simply centering the uplink beacon image in the camera frame would ensure that the downlink beam was centered on the ground station receiver. However, the camera and downlink beam aperture are not perfectly aligned. Additionally, environmental effects have the potential to change the alignment, especially during launch (when vibrational loads are highest) and prior to installation on the ISS (when thermal fluctuations are highest). A plan to compensate for the bias after OPALS is installed on the ISS is needed because the alignment could change post-verification

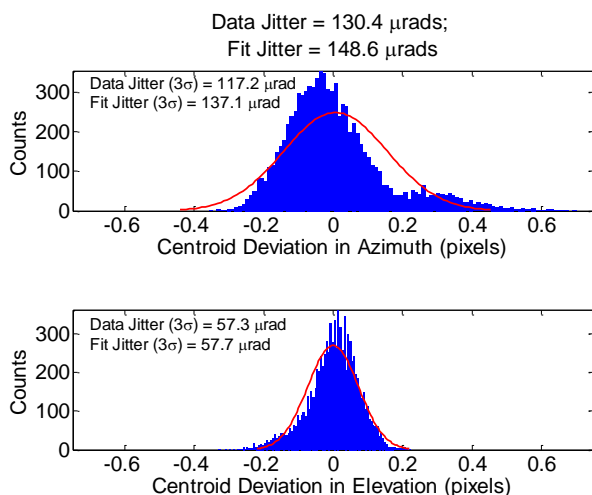


Fig. 6. Downlink jitter is measured indirectly from the movement of the ground beacon (at the acquisition threshold) on the Flight System camera CCD. The histograms show the residual error, in pixels, from the centroiding algorithm in the azimuth [top] and elevation [bottom] axes for a representative closed-loop tracking test. A Gaussian fit to the data is shown in red. The jitter could be computed from either the histogram itself or from the fit, although neither provides the most accurate estimation of the impact on the link.

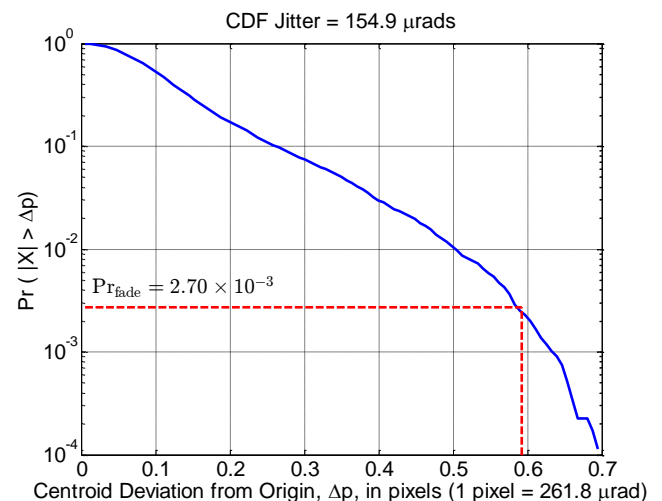


Fig. 7. Cumulative density function (CDF) plots showing the total measured jitter. The CDF allows us to estimate the effective jitter based on deviation at which the probability of a fade is equal to that one would obtain with a Gaussian distribution, i.e., $\text{Pr}_{\text{fade}} = 2.7 \times 10^{-3}$.

on the ground.

OPALS makes use of a system capability called ‘centroid deviation’ in order to estimate and correct the effects of misalignment of the camera and downlink beam aperture. A centroid deviation is simply a software-defined, time-varying offset introduced during closed-loop tracking. Nominally, this value is zero in the native coordinate system used to address the camera sensor, and consequently the centroid is at the center of the camera image. If instead, we wanted to hold the centroid off-center by N pixels, we can introduce a centroid deviation of N . We can correct for a misalignment between the tracking camera and the downlink beam aperture by including an equal and opposite centroid deviation. For example, if the misalignment between the tracking camera and the downlink beam aperture were known to be 2.62 mrad in the +X direction with respect to the camera image, OPALS could correct for the misalignment by including a centroid deviation of 10 pixels in the -X direction, given that a centroid deviation of one pixel corresponds to an angular deviation of 261.8 μ rad. If the misalignment is not known—as is the case when OPALS becomes operational on the ISS—then we resort to a centroid deviation scan to estimate the bias.

The object of the OPALS Flight-Ground Calibration Scan (FGCS) is to use a time-varying centroid deviation table to effectively sweep the beam over the ground receiver in a known pattern and look at the power of the received signal to back out the misalignment. We can command the sweep rate, so the time it takes to complete the scan pattern is known. For testing this approach, a raster scan trace similar to that shown in Fig. 8 is used. We begin the scan at (-X,-Y) and hold our Y-value constant, sweeping to (+X, -Y). Then, we jump to (+X, -Y+ ΔY) and sweep (-X, -Y+ ΔY). This pattern continues until we complete a full trace and end at (+X, +Y). Then, we repeat the scan in reverse scanning from (+X, +Y) to (-X, -Y). We do this complete there-and-back scan as many times as possible within a 110 second pass window. If the misalignment falls within the scan, then at some point, the ground receiver will see power fluctuations that give us information about what the misalignment is and how we can correct for it in future pass attempts.

The OPALS FGCS was validated with the integrated Flight System and the Ground Station Emulator. A pin-hole aperture (with a diameter of 25 μ m) was placed in front of the receiver. The flight laser spot size at the aperture was calculated to be 15-20 mm. The ratio of beam size to pin-hole diameter is $\sim 700 \pm 100$. This is meant to mimic the ratio of the flight laser spot size on the ground and the 1 m receiving telescope. With a 1.08 mrad beam divergence, the experimental ratio is reasonably close to the expected flight ratio of 630-1260 (depending on the range of the ISS at 350 km and 700 km, respectively). The flight laser was operated at full output power.

Looking at Fig. 9 we can see the power recorded by the Ground System emulator. In this test, the beam spot size is estimated to be 15-20 mm at the 25 μ m pin-hole. Thus, for each sweep from (-X,-Y) to (+X,+Y), we would expect to see several peaks in the received power, as is the case in Fig. 9 (Top). There are 12 sweeps in the Y (or elevation) direction.

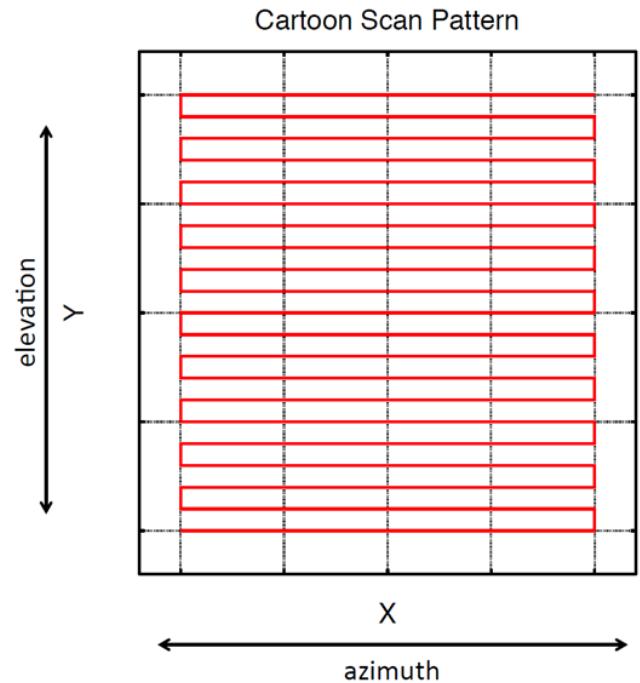


Fig. 8. Cartoon representation of a FGCS raster pattern used in OPALS verification testing. The raster begins at (-X,-Y) and the scan sweeps the total range of X, and then makes a short step in Y. This process is repeated until the sweep covers the entire range at (X,Y). Then, the sweep reverses direction and follows the same path backwards to (-X,-Y). The FGCS continually follows this zig-zag pattern of sweeping and backwards re-trace for the duration of the calibration event. For OPALS validation testing, the scan was a square centered at the camera CCD origin with sides 14 pixels long (equivalent to 3753.4 μ rad) and with steps in the Y direction of 0.1865 pixels (50 μ rad). A sweep begins at (-7,-7) pixels and ends at (7,7) pixels.

Within each of these 12 sweeps, we can see individual peaks as the beam sweeps in the X (azimuth) direction (Fig. 9 Middle and Bottom panels). In the top panel of Fig. 9, we can see the time between peaks (labeled Δt_1 and Δt_2). If there were no misalignment in the Y direction, Δt_1 and Δt_2 would be equal. If there is an offset, then we would expect to observe all durations labeled Δt_1 to be equal and all durations labeled Δt_2 to be equal, but Δt_1 and Δt_2 would not be equal to each other. We can solve for the absolute value of the Y-component of misalignment ($|\mathbf{M}_y|$) from the center of the camera CCD using,

$$|\mathbf{M}_y| = \mathbf{V}_y \frac{|\Delta t_1 - \Delta t_2|}{2}. \quad (1)$$

Here \mathbf{V}_y is the velocity that the optical head sweeps in the Y-direction. For the results shown in Fig. 9, $\mathbf{V}_y = 1.554$ pixels/s (416.63 μ rad/s), $\Delta t_1 = 8.4410 \pm 0.0453$ s, and $\Delta t_2 = 8.8498 \pm 0.0370$ s. Duration errors are one standard deviation of the sample. Therefore, we estimate $|\mathbf{M}_y| = 0.318 \pm 0.007$ pixels (85.256 ± 1.877 μ rad). Knowing that the sweep begins at -Y, goes to +Y, and back, we know that this offset is in the positive Y direction. We can perform a similar analysis for the X-

component of misalignment (\mathbf{M}_x) from the center of the camera CCD using,

$$|\mathbf{M}_x| = \mathbf{V}_x \frac{|\delta t_1 - \delta t_2|}{2}. \quad (2)$$

Here \mathbf{V}_x is the velocity that the optical head sweeps in the X-direction. For the results shown in Fig. 9, $\mathbf{V}_x = 116.667$ pixels/s (31.278 mrad/s), $\delta t_1 = 0.1107 \pm 0.0026$ s, and $\delta t_2 = 0.1166 \pm 0.0023$ s. Duration errors are one standard deviation of the sample. Therefore, we estimate $|\mathbf{M}_x| = 0.344 \pm 0.018$ pixels (92.226 ± 4.826 μ rad). Since the X sweeps are so much faster than the Y sweeps and we do not have sufficient timing synchronization, we cannot tell if the X-component of the misalignment is in the positive or negative X direction. After completing one FGCS in orbit, the OPALS operators could choose to accept the X-component uncertainty (~ 194 μ rad in this case). Alternately, the operators could try the scan again with the raster pattern rotated by 90 degrees. This rotation would allow for slower sweeps in the X-direction and the sign the X-component of misalignment could be extracted in the same way as the Y-component in the example illustrated here.

By taking the root-sum-square of the X- and Y-components, we obtain our estimate of the bias to be approximately 200 μ rad. This test, therefore, would suggest that the 150 μ rad pointing bias requirement is exceeded by about 50 μ rad. The project has deemed this to be acceptable since the overall mispoint allocation of 525 μ rad is met due to the better-than-expected jitter performance. It is also anticipated that repeating the FGCS during operations several times could improve the bias estimation sufficiently to bring it in compliance with the requirement. At this time, conservative estimates of the combined jitter and bias contributions put the total anticipated mispoint at 400 μ rad.

The FGCS technique was designed to determine the misalignment between the OPALS tracking camera and downlink laser aperture. Alternate methods that necessitated timing synchronization between the Flight System and the Ground System were investigated. However, without a dedicated GPS clock or accurate knowledge of latencies aboard the ISS and the Flight System, we could not assure the time synchronization required. One potential drawback of the FGCS method is that the power received at the Ground Station will vary as a function of distance from the ISS during a pass. However, over the course of several seconds, i.e. a sweep of the beam past the pin-hole in Fig. 9 (Bottom), the power fluctuations should be small enough that our method for determining local maxima in the power received by the receiver will still provide an acceptable approximation of the true misalignment.

IV. CONCLUSIONS

In this paper we have presented the effects of the OPALS pointing performance on the optical downlink. We began by describing how the pointing-induced losses are defined and how allocations were made based on acceptable levels of pointing-induced fades given per the photon budget. We have

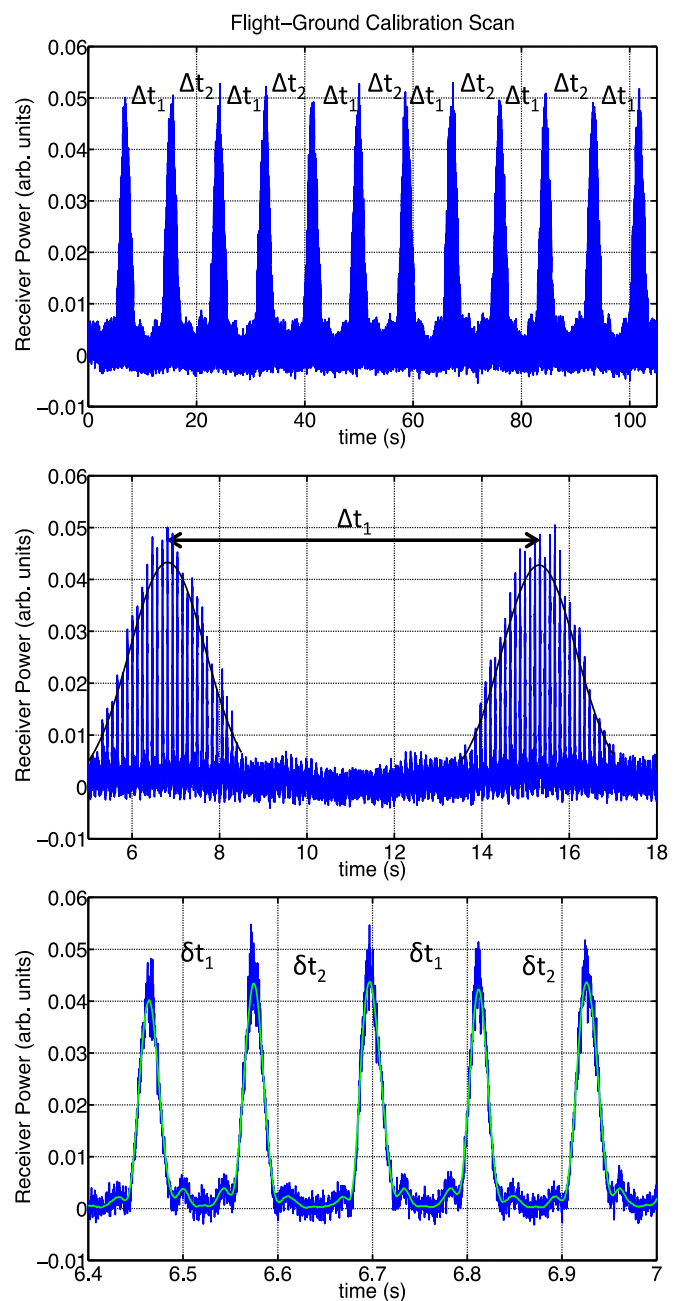


Fig. 9. Power received at the ground system emulator with the pin-hole as a function of time. Top: All 105 seconds of a FGCS test. This test consisted of six complete sweeps from (-7,-7) pixels to (7,7) pixels and back. There are 12 total sweeps in the Y direction (6 up and 6 down). Increments of time labeled Δt_1 and Δt_2 represent the time between local maxima power recorded on the receiver. Middle: Same as top, but a limited time range between 5 and 18 seconds. Gaussian fits (black) to smoothed power data (smooth not shown in middle panel) indicate the time of local maximum power for the first two Y sweeps. Bottom: Same as above for a time range between 6.4 and 7 seconds. A smoothed power time series (green) is shown. The time between subsequent local maxima are given by either δt_1 or δt_2 .

identified that the power delivered to the ground detector is most sensitive to the combination of jitter sub-allocation and beam width design. We then presented our methodology for

testing the jitter performance of the fully-integrated Flight System, as well as a flight-ground calibration scan technique used to estimate the bias post-installation on the ISS. Laboratory testing revealed that the jitter performance could be a factor of 2.2 better than the requirement, while the bias requirement could be exceeded by about 33%. The overall mispoint allocation, however, is still met by 20-25%, thus providing confidence that the overall pointing performance of the OPALS system is more than sufficient to enable a high-quality optical downlink.

ACKNOWLEDGMENT

The authors express their appreciation to all project members, past and present, for their commitment to the OPALS project through its development and operations. The authors acknowledge all of the OPALS team members, whose technical contributions made the writing of the paper possible.

REFERENCES

- [1] National Aeronautics and Space Administration, "Optical Payload for Lasercomm Science (OPALS)." <http://www.nasa.gov/mission_pages/station/research/experiments/861.html> (14 March 2014).
- [2] B.V. Oaida, M.J. Abrahamson, R.J. Witoff, J.N.B. Martinez, D.A. Zayas, "OPALS: An optical communications technology demonstration from the International Space Station," IEEE Aerospace Conference, pp.1-20, March 2013
- [3] B.V. Oaida, W. Wu, B.I. Erkmen, A. Biswas, K.S. Andrews, M. Kokorowski, M. Wilkerson, "Optical link design and validation testing of the Optical Payload for Lasercomm Science (OPALS) system," *Proc. SPIE*, Free-Space Laser Communication and Atmospheric Propagation XXVI, vol. 8971, no. 89710U, pp 1-15, March 2014
- [4] H. Hemmati, A. Biswas, I.B. Djordjevic, "Deep-Space Optical Communications: Future Perspectives and Applications," in *Proceedings of the IEEE*, vol.99, no.11, pp.2020-2039, 2011.